A Numerical Investigation of the Down-Valley Flow Regime Observed during EOP 4 of T-REX 2006

Robert E. Dumais, Jr * (1) and Sen Chiao (2)

(1) U.S. Army Research Laboratory, White Sand Missile Range, NM
(2) Marine and Environmental Systems, Florida Institute of Technology, Melbourne, FL

.

1. Introduction

Down-valley flow is often observed to pulse in strength and to be very turbulent. During nocturnal cooling periods, if relatively weak synoptic winds and minimal cloud coverage are observed, the development of a stable (nocturnal) boundary layer begins. As the surface continues to cool through radiative heat loss, a layer of warmer temperatures elevates as the surface longwave radiation cooling progresses. Temperatures at the surface will continue to cool until sunrise, yielding a minimal temperature value near that time. Nocturnal down-valley flows develop when the katabatic (buoyant) acceleration, due to the near-surface air cooling exceeds the opposing along-slope pressure gradient (e.g., Pinto et al., 2006, Whiteman and Zhong 2008, Papadopoulos and Helmis 1999). Banta and Cotton (1981) used the term "wind regime" as a generic term to include wind systems forced by similar mechanisms. Three regimes are defined in the paper: 1) the upslope regime including both upslope and upvalley winds for which the ultimate cause is heating of the surface; 2) the downslope regime including both drainage and down-valley winds; 3) the regime of the afternoon wind system caused by convective mixing as the surface winds result from the downward mixing of momentum within the deep afternoon convective boundary layer (CBL).

Whiteman (1990) reviewed observational evidence, concentrating on the thermal changes in rather steep-sided valleys. Four regimes within the diurnal cycle of a valley wind system are categorized by Whiteman, which include nighttime, morning transition, daytime, and evening transition. The thermal structure of the nocturnal valley atmosphere has also been elucidated by the observational studies of Triantafyllou et al. (1995) and Whiteman et al. (1996). Some other nocturnal airflows in valleys have been widely observed, such as those reported by Clements et al. (1989). The depth and strength of down-valley flows in different valleys is related to the size of the drainage source regions and may interact with other mesoscale circulations such as lake breezes (e.g., Zumpfe and Horel 2007).

In this study, we focus our investigation upon the numerical simulation of a down-valley flow regime established under a stable boundary layer condition. We will examine the case of Enhanced Observing Period (EOP) 4 during the spring 2006 Terrain-induced Rotor Experiment (T-REX), where an extended stable boundary condition was observed throughout the night and early morning hours of April 28-29. The T-REX field campaign was held during March and April of 2006 in the Owens Valley of southeastern California. Its main objective was to study the coupled mountain-wave, rotor, and boundary-layer system under highly perturbed atmospheric states, with a secondary objective to evaluate the stratospheric-tropospheric structure and evolution of the complex terrain boundary layer during more quiescent conditions (without rotors present). A goal of T-REX is to use the collected field observation data to help in the validation of numerical models, improve mesoscale and microscale modeling, and help better predict aviation hazards, down slope windstorms, and aerosol transport and dispersion (Grubisic et al, 2008).

2. Brief overview

The Owens Valley surrounds the Owens River located in southeastern California, and is roughly 20 km wide (west to east) and 120 km long (north to south). The valley is surrounded by the Sierra Nevada Mountains to the west and both the Inyo and White Mountains to the east. Both the White and Sierra Nevada mountains have peak elevations above 4 km (14,000 ft), while the Inyo Mountains contain a peak of over 3.3 km (11000 feet). The Owens Valley itself is a relatively elevated valley at 1.2 km (4,000 ft) above sea level, but due to the extreme heights of the mountain ranges on both sides it is in fact one of the deepest valleys in the United States. The Sierra Nevada Mountains are also one of the tallest and steepest topographic barriers in the United States, giving way to extreme and interesting atmospheric phenomenon. The marine environment not too far west in proximity to the arid continental desert climate of the region also provides for interesting local meteorological conditions.

The EOP 4 of the T-REX was conducted from 2300 UTC 28 to 2000 UTC 29 April 2006. The high resolution GOES-10 visible satellite imagery from 2330 UTC April 28 showed no prominent cloud field over the Owens Valley at this time, although there was a little afternoon convective cloud development over particularly the Sierra Nevada Mountains to the west. On the afternoon of April 28, the convergence evidenced along the peaks of the Sierra Nevada appears to be enhanced by the well-developed afternoon upslope winds arriving from the valleys on both sides of the range. The synoptic weather conditions during the observational period were governed by (1) a mid-level ridge axis that passed over the Owens Valley by 1200 UTC 29 April 2006 and (2) a surface area of lower pressure that was observed near the southern end of the Owens Valley.

The vertical velocity and wind profiles observed by the NCAR Integrated Sounding System (i.e., ISS2; 1475 m above sea level) operated within the Owens Valley demonstrated that weak upward motion (0.2 ~ 1 m s^{-1}) dominated the Owens Valley boundary layer during much of the period through about 1800 UTC 29 April around this site. It has been theorized that the ISS2 vertical motion and horizontal wind fields observed above about 1.5 km above ground level (agl) between 0500 UTC- 1200 UTC 29 April were contaminated by the extended flight pattern of migratory nocturnal birds (not shown), so the profiler observations may not represent the real situation at that time (Schmidli, Personal Communication) for that approximate height level. High ISS2 profiler signal-to-noise ratios observed at these same levels/times are good indicators that such contamination may have occurred, along with the fact that nearby University of Leeds' soundings do not show the same wind structure between roughly 1.5- 3 km agl. Overall, the upward motion over the valley floor was much less than 1 m s^{-1} just before the sunrise, and the profiler indicates that a convective boundary layer formed shortly after sunrise. Early during the period there were prevailing northwesterly winds of 5-10 m s^{-1}, which slowly abated with both increasing time and height over the Owens Valley. .

3. Model description and experimental design

Numerical simulations were performed using the WRF-ARW version 3 (Skamarock et al., 2008). The advanced research WRF dynamical core is based on a Eulerian solver for the fully compressible, non-hydrostatic equations with a hydrostatic option. Variables are solved in the scalar-conserving flux form. The vertical coordinate is a mass-based terrain-following coordinate, and the horizontal/vertical grid staggering is done on an Arakawa C-grid. The Runge-Kutta third-order time scheme as well as fifth and third order advection schemes are adopted in the horizontal and vertical directions, respectively (Wicker and Skamarock 2002). A time-split integration scheme is used on a shorter time-step for the acoustic and gravity-wave modes. Detailed information about the WRF model may be found at: www.wrf-model.org.

A double-nested simulation of the WRF-ARW model was configured with grid spacings of 4.5 km (121 x 121) and 1.5 km (169 x 169) for domain 1 and domain 2, respectively. Figure 1 shows the configuration of domains and topography features in the nested domain. The top of the atmosphere in the model is located at the 50 hPa level, and a total of 60 unequally spaced terrain-following levels in the vertical are employed. The initial cold start and the time-dependent lateral boundary conditions are both derived from the North American Mesoscale model (NAM-218, i.e., 12 km grid spacing) forecasts from the National Center for Environmental Prediction (NCEP). A 36-hr simulation was conducted starting at 1200 UTC 28 April 2006, which allowed enough spin-up time (at least 10 hrs) for the model results to be reasonably evaluated throughout the duration of the down-valley jet (DVJ) cycle of EOP4.

The planetary boundary layer scheme used in this study is the Quasi-Normal Scale Elimination (QNSE) scheme which is developed for stable and weakly unstable stratification conditions and is a new option in WRF-ARW. This scheme accommodates the stratification-induced disparity between the transport processes in the horizontal and vertical directions and accounts for the combined effect of turbulence and waves. The vertical turbulent viscosity (K_M) and eddy diffusivity (K_H) can be normalized by eddy viscosity of neutral turbulent flow (K_0) and presented as functions of the local gradient of Richardson number (Ri). Details of the QNSE theory are described in Sukoriansky et al. (2005, 2006) and Galperin et al. (2007). The atmospheric radiation scheme accounts for longwave (Mlawer et al. 1997) and shortwave transfers and interactions with the atmosphere, clouds, and the surface (Dudhia 1989).

No cumulus scheme was used on either grid, and precipitation (if any) was produced from explicit grid-scale condensation and convection. The Thompson microphysical parameterization (Thompson et al. 2004) was used in this study. The NOAH land-surface model option was also incorporated. The discussions to follow will concentrate on the inner 1.5 km resolution domain results, and in this short extended abstract focus mostly on the surface flow behavior. A more detailed manuscript discussing the full experiment and analysis is being prepared for open literature publication.

4. **The evolution of the valley surface flow field in EOP4**

Owens Valley meteorological analyses derived from the T-REX soundings, profilers, and surface station observations clearly show that a down-valley surface flow regime initiated during the local afternoon of 28 April 2006 and persisted through the local morning of 29 April 2006. Figures 2-5 show the observed surface wind and temperature fields across the valley at several different times during the Apr 28-29 EOP4 period (composited from mesonets and HOBOs), while Figures 6-9 show model simulated 10-m wind and 2-m temperatures for these same times on the 1.5 km grid spacing nest. On 2200 UTC 28 April, the simulated north-northwesterly flow is about 5~10 m s^{-1} in the valley. Some weak upslope flows are also found along both sidewalls of the Valley. The stronger temperature gradients that were observed along the slopes of both the Sierra Nevada and the Inyo were well simulated.

Within the valley, the simulated surface temperatures were about 29.5 ^{o}C, while near the tops of the highest mountains in the Sierra Nevada they are less than 10 ^{o}C in some areas (resulting in a lapse rate near 6.5 ^{o}C/1000 m). A noteworthy feature is that the highest temperature (>32 ^{o}C) was simulated within the basin-shaped Saline Valley to the east of the Inyo Mountains, although no observational data is available to validate this finding. Compared to the observed DRI surface station temperatures, the model was generally about 1^{o}C colder in the valley during this time.

Six hours later at 0400 UTC 29 April, the simulated result clearly shows the establishment of downslope/drainage winds from the mountain slopes on both sides of the valley, along with a line of surface wind convergence along the east side of the valley. The model surface temperature of the valley dropped about 8 ^{o}C within the 6 hours, with the simulated valley temperature field still generally about 1 ^{o}C colder than the observed. However, around the location of the town of Independence, there is a small area where winds dropped to below a few knots and temperatures plummeted almost 15 º C over the period 0100 UTC to 0400 UTC. In this same area, this winds increased after 0500 UTC and the temps recovered several degrees by 0700 UTC (and then dropped steadily again through about 1400 UTC). The model winds did not sufficiently weaken enough during this period to accurately reproduce this localized short-term cool pool around 0300-0500 UTC.

By 1200 UTC 29 April, the model was able to capture the downslope flow (~ 5 m s^{-1}) observed by mesonet stations on the westernmost sidewall of the valley, as well as the downslope flow (~ 10 m s^{-1}) over the mesonet sites on the eastern sidewall of the valley. In addition, the simulated surface heat fluxes (not shown) over the valley were -76 W m^{-2} at 1200 UTC 29 becoming 57 W m^{-2} at 1500 UTC 29 April, and over the eastern slopes was -67 W m^{-2} at 1200 UTC 29 becoming 99 W m^{-2} at 1500 UTC 29 April. It appears the radiative heating over much of the valley floor and especially the eastern slopes of the Sierra Nevada was much faster than over the western slopes of the Inyo at this time. The local topographical induced flow observed at the foothills of the Inyo Mountains is also reasonably simulated by the model, as is the prevailing down-valley regime which eventually dominated. It also appears that some adiabatic warming associated with the strong surface drainage winds existed along the foothill of the east sidewall in the Valley. The two opposing drainage-type flows seem to bec0me confluent near the mesonet surface stations and evolved into a more steady, widespread, and general down-valley flow pattern as the night progressed.

By 1800-2100 UTC 29 April, the early development of the upslope winds (observed) on both sidewalls of the valley are simulated. The model surface temperatures are in decent agreement with those observed. By this time on 29 April, the down-valley wind regime had weakened significantly. The model did appear to have recaptured the relative timing of the transition period to up-valley from down-valley wind flow, which based upon the observations occurred first near the southern part of the Owens Valley around or just after 1800 UTC 29 April (Fig. 8d).

Overall, at the surface the model appears during EOP4 to have simulated the complete down-valley flow evolution properly, including some of the more complicated aspects associated with the valley flow transition periods. It is also apparent from this case study that the model surface temperatures in the valley can still be improved upon, especially in the evening transition hours. Although not shown here due to space limitations, the upper air/ three dimensional characteristics of the nocturnal boundary layer and down-valley jet structure were also simulated quite reasonably. For example, the demarcation zone above the valley floor separating the DVJ regime from the synoptic flow was well captured, as were the transitions from convective to stable boundary layer structures.

In the future (but outside the scope of this study) we may investigate the sensitivity of the model to choice of surface layer and land surface schemes, in addition to looking at how improved land use, soil moisture and snow cover initialization could impact results. For example, initial snow cover fields erroneously interpolated onto valley grid point locations (say, at 1 km grid spacing) from NAM 218 output could certainly negatively impact modeled valley heating rates and the subsequent diurnal wind regime simulations.

5. Conclusion

This study is focused upon modeling a down-valley flow case associated with a nocturnal stable boundary condition, which occurred during the T-REX field experiment throughout the EOP4. This case provided an excellent opportunity to study the processes that lead to the variation of the strength and depth of such valley flow under relatively dry and weak synoptic conditions. It also offered a great opportunity to better assess the ability of the fine resolution WRF-ARW model in conjunction with a newly developed planetary boundary layer scheme for stable conditions (i.e., QNSE) to replicate the nocturnal stable boundary condition. We examined the role of the down-valley flow in association with the diurnal variation of the along-valley/slope wind system, as well as investigating what enhances their formation. This was accomplished through the use of both in situ EOP4 field measurements and the WRF-ARW high resolution numerical simulations.

During EOP4, a strong northerly down-valley jet (~ 10 m s^{-1}) occurred throughout the evening after 0400 UTC 29 April under the influence of a mostly N-S meridional synoptic flow. Additionally, the nocturnal DVJ was affected by the diurnal mesoscale heating/cooling regime throughout the Owens Valley, and the topography effects from both sidewalls of the valley due to the bounding Sierra Nevada and Inyo Mountains. By the afternoon of 29 April 2006, synoptic high pressure began to entrench itself over the region and a reversal to southerly up-valley flow became evident by 2100 UTC 29 April 2006. The numerical experiment shows that the mean diurnal flow behavior of the Owens Valley is captured by the WRF-ARW inner nest 1.5 km grid spacing results, comparing well with the NCAR ISS2, University of Leeds' radiosonde soundings from the Independence airport, and the DRI surface mesonet results (and also with the University of Leeds' AWS and University of Utah surface HOBO observations).

References

Banta, R., and W.R. Cotton, 1981: An Analysis of the Structure of Local Wind Systems in a Broad Mountain Basin. J. Appl. Meteor., 20, 1255–1266.

Clements, W.E., J.A. Archuleta, and P.H. Gudiksen, 1989: Experimental Design of the 1984 ASCOT Field Study. J. Appl. Meteor., 28, 405–413.

Dudhia, J., 1989: Numerical study of convection observed during the winter monsoon experiment using a mesoscale two-dimensional model. J. Atmos. Sci., 46, 3077-3107.

Galperin B., S. Sukoriansky, V. Perov, 2007: Implementation of the quasi-normal scale elimination (QNSE) turbulence model in WRF. The 8th WRF Users' Workshop, Boulder, CO, June 11-15, 2007.

Grubišić, V., J. D. Doyle, J. Kuettner, S. Mobbs, R. B. Smith, C. D. Whiteman, R. Dirks, S. Czyzyk, S. A. Cohn, S. Vosper, M. Weissmann, S. Haimov, S. F. J. DeWekker, L. L. Pan, F. K. Chow, 2008: The Terrain-induced Rotor Experiment: An overview of the field campaign and some highlights of special observations. Bull. Amer. Meteor. Soc., 89, 1513-1533.

Mlawer, E. J., S. J. Taubman, P.D. Brown, M. J. Iacono, 1997: Radiative transfer for inhomogeneous atmospheres: RRTM, a validated correlated-k model for the longwave. J. Geophys. Res. Vol. 102, 16663-16682.

Papadopoulos, K. H. and Helmis, C. G., 1999: Evening and morning Transition of katabatic Flows. Boundary-Layer Meteorol. 92, 195-227.

Pinto, J.O., D.B. Parsons, W.O.J. Brown, S. Cohn, N. Chamberlain, and B. Morley, 2006: Coevolution of Down-Valley Flow and the Nocturnal Boundary Layer in Complex Terrain. J. Appl. Meteor. Climatol., 45, 1429–1449.

Schmidli, J., 2007: Personal Communication.

Skamarock, W. C., J. B. Klemp, J. Dudhia, D. O. Gill, D. M. Barker, M. Duda, X.-Y. Huang, W. Wang and J. G. Powers, 2008: A Description of the Advanced Research WRF Version 3, NCAR Technical Note, 2008.

Sukoriansky, S., B. Galperin and I. Staroselsky, 2005: A quasi-normal scale elimination model of turbulent flows with stable stratification. Physics of Fluids, 17, 85-107.

Sukoriansky, S., B. Galperin, and V. Perov, 2006: A quasi-normal scale elimination model of turbulence and its application to stably stratified flows. Nonlinear Processes in Geophysics, 13, 9-22.

Thompson, G., R. M. Rasmussen, K. Manning, 2004: Explicit forecasts of winter precipitation using an improved bulk microphysics scheme. Part 1: Description and sensitivity analysis. Mon. Wea. Rev.. 132. 519-542.

Triantafyllou, A. G., Helmis, C. G., Asimakopoulos, D. N. and Soilemes, A. T.: 1995, 'Boundary layer evolution over large and broad mountain basin', Theor. Appl. Climatol. 52, 19–25.

Whiteman, C. D., 1990: Observations of thermally developed wind systems in mountainous terrain. Atmospheric Processes over Complex Terrain, Meteor. Monogr. No. 45, Amer. Meteor. Soc., 5–42.

Whiteman, C.D., and J.C. Doran, 1993: The Relationship between Overlying Synoptic-Scale Flows and Winds within a Valley. J. Appl. Meteor., 32, 1669–1682.

Whiteman, C. D., T. B. McKee, and J. C. Doran, 1996: Boundary layer evolution within a canyonland basin. Part I. Mass, heat, and moisture budgets from observations. J. Appl. Meteor. 35, 2145-2161.

Whiteman, C. D., and S. Zhong, 2008: Downslope flows on a low-angle slope and their interactions with valley inversions. Part I. Observations. J. Appl. Meteor. Climat., 47, 2023-2038.

Wicker, L. J., and W. C. Skamarock, 2002: Time splitting methods for elastic models using forward time schemes. Mon. Wea. Rev., 130, 2088-2097

Zumpfe, D.E., and J.D. Horel, 2007: Lake-Breeze Fronts in the Salt Lake Valley. J. Appl. Meteor. Climatol., 46, 196–211.

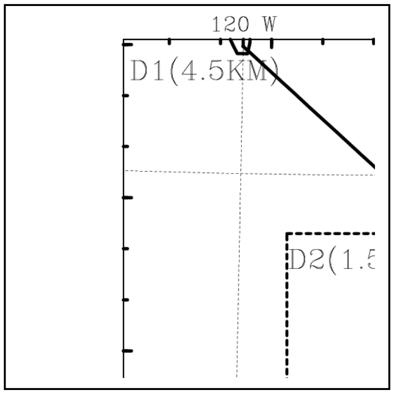

Figure 1. WRF-ARW 4.5 and 1.5 km grid spacing nests used in simulation.

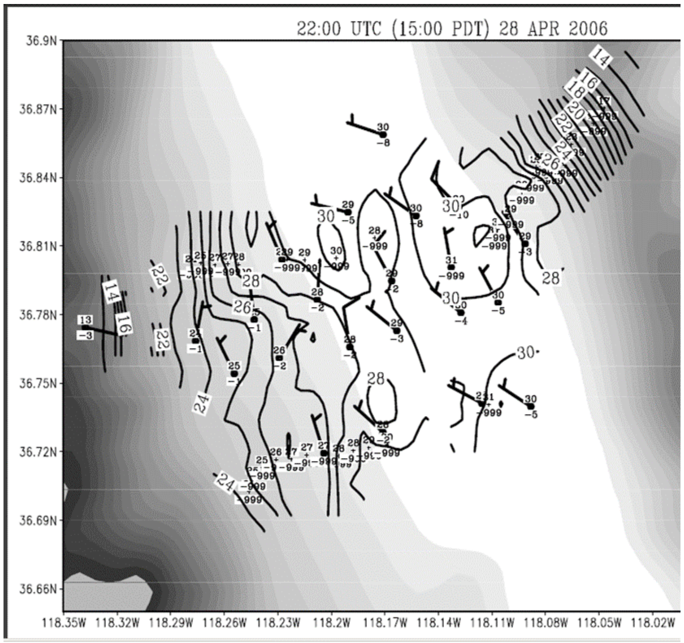

Figure 2: Objective analysis of surface mesonet observations over Owens Valley at 2200 UTC 28 Apr 2006.

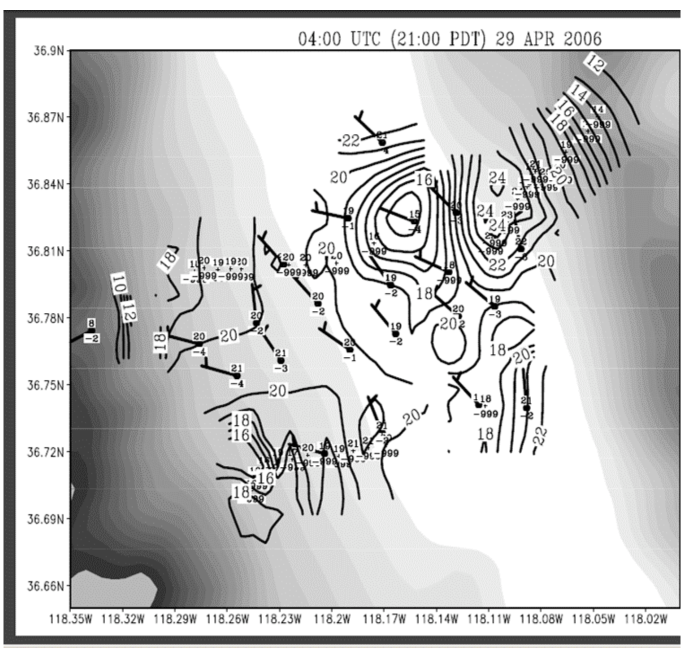

Figure 3: Objective analysis of surface mesonet observations over Owens Valley at 0400 UTC 29 Apr 2006.

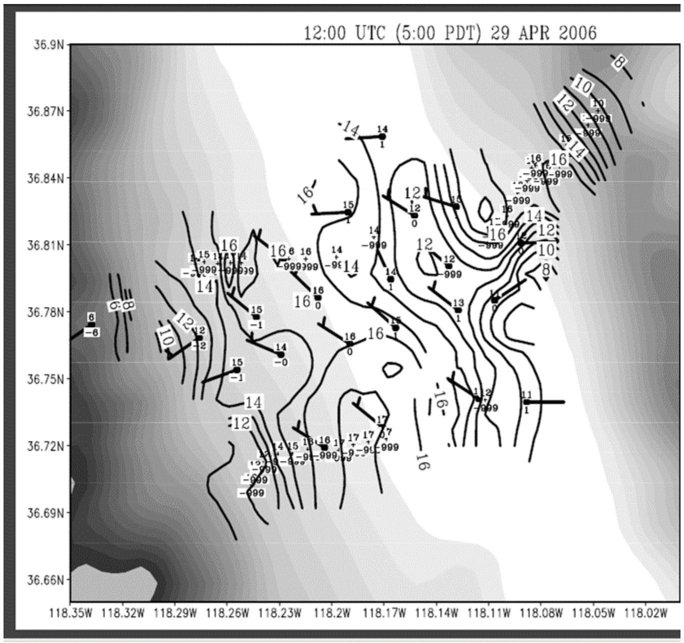

Figure 4: Objective analysis of surface mesonet observations over Owens Valley at 1200 UTC 29 Apr 2006.

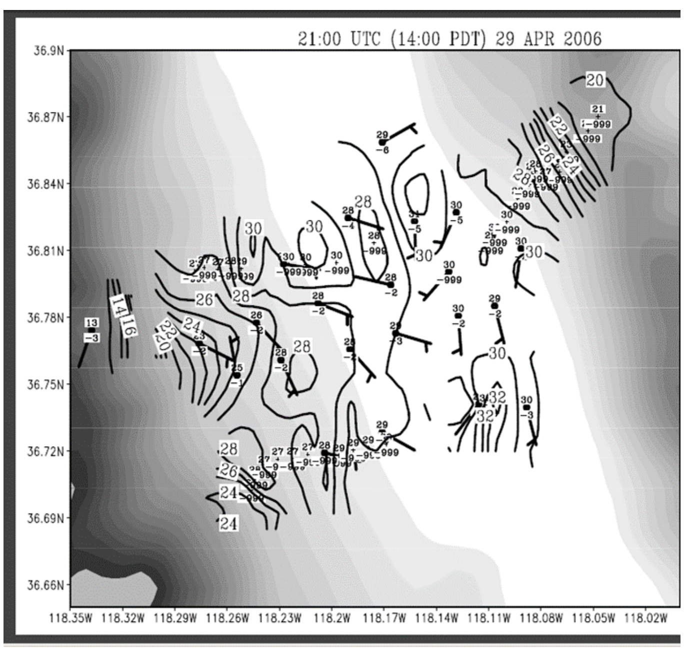

Figure 5: Objective analysis of surface mesonet observations over Owens Valley at 2100 UTC 29 Apr 2006.

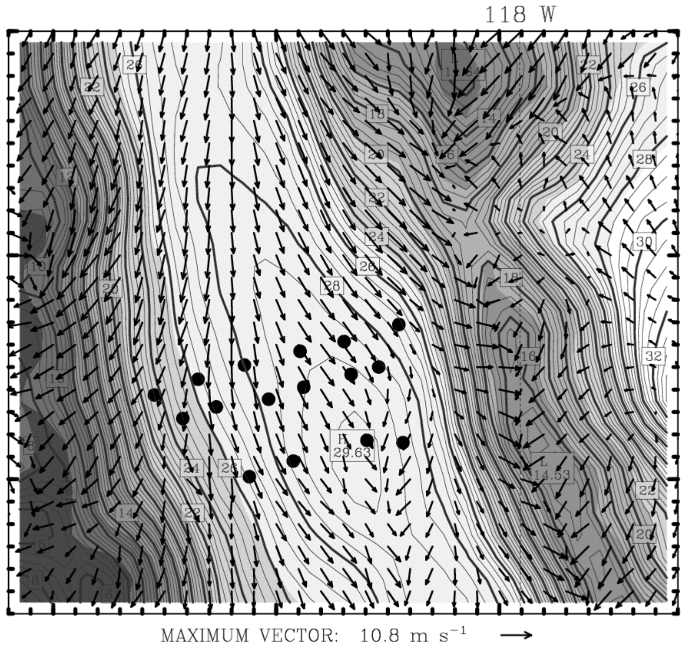

Figure 6: WRF-ARW 1.5 km nest surface forecast valid at 2200 UTC 28 Apr 2006 (black dots are Desert Research Institute's mesonet locations).

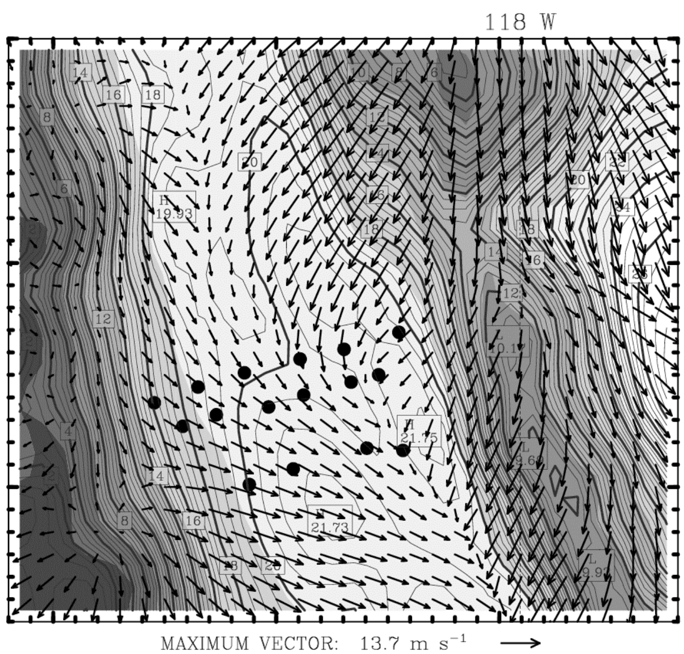

Figure 7: WRF-ARW 1.5 km nest surface forecast valid at 0400 UTC 29 Apr 2006 (black dots are Desert Research Institute's mesonet locations).

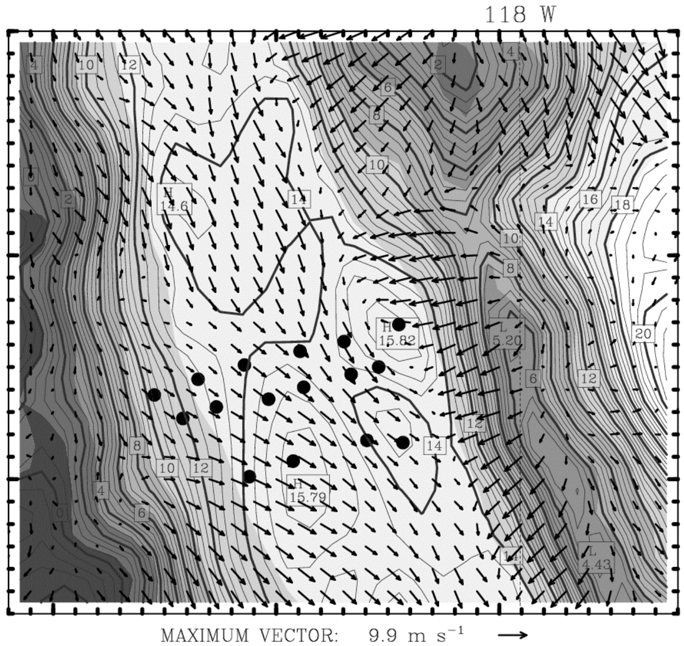

Figure 8: WRF-ARW 1.5 km nest surface forecast valid at 1200 UTC 29 Apr 2006 (black dots are Desert Research Institute's mesonet locations).

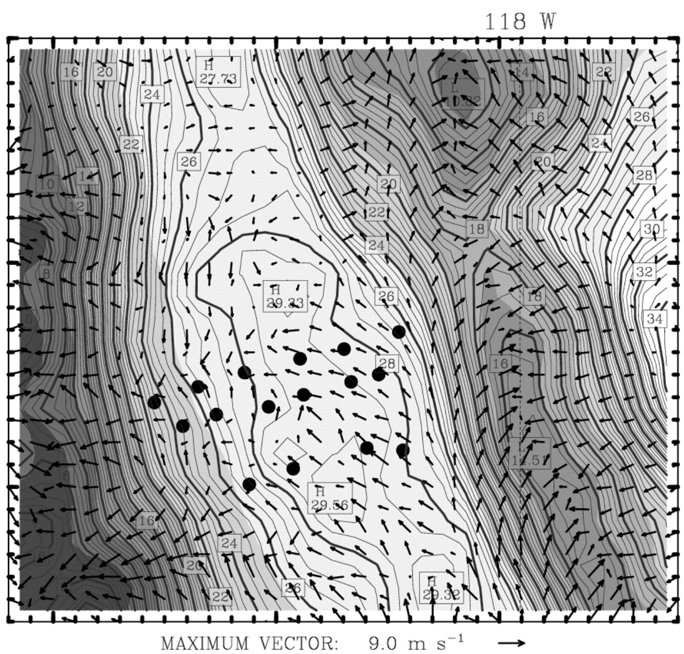

Figure 9: WRF-ARW 1.5 km nest surface forecast valid at 2100 UTC 29 Apr 2006 (black dots are Desert Research Institute's mesonet locations).